TABLE IV. Field gradients (in units of 10^{21} cm^{-3}) in *Al*-Zn and *Al*-Mg.

Shell	1	2	3	4	5	6	7
Zn	79	4.1	4.8	4.7	8.1	6.1	1.5
Mg	45	26	12	5	10	8.4	6.5

around the impurity, using an elastic model,[21] modifies only slightly the theoretical values. The improved resistivity values we have used do not, in fact, produce any better agreement with the experimental results.

In *Al*-Ag, *Al*-Si, and *Al*-Ge, the values of $\Delta\rho$ furnish several estimates of δ_0 and δ_1, but in each case the disagreement with the experimental results is complete.

It would be worthwhile to use a method with greater validity at the level of the first neighbors, for example by taking into account a preasymptotic term[26] in R^{-4}, or else by treating simultaneously the size and charge effects of the impurity as has been done by Beal-Monod and Kohn.[27]

ACKNOWLEDGMENTS

The author would like to express his thanks to Dr. P. Averbuch for his continuing encouragement and stimulating conversations. He is also grateful to Dr. M. Goldman, Dr. J. Levin, and C. Berthier for their helpful suggestions and discussions, and to R. Andreani for his assistance in the experiments. He is indebted to Dr. Bethoux, of the Centre de Recherches sur les Très Basses Température de Grenoble, for the preparation of the samples, and to Dr. J. P. Morlevat, of the Metallurgy section of the Centre d'Etudes Nucléaires de Grenoble, for the microprobe analyses.

[26] L. C. R. Alfred and D. O. Van Ostenburg, Bull. Am. Phys. Soc. **11**, 45 (1968).

[27] M. T. Beal-Monod and W. Kohn, J. Phys. Chem. Solids **29**, 1877 (1968).

PHYSICAL REVIEW VOLUME 182, NUMBER 2 10 JUNE 1969

Microwave Spectroscopy of OH^- Ions in the KCl and NaCl Lattices*

R. S. SCOTT AND W. H. FLYGARE
Materials Research Laboratory and Noyes Chemical Laboratory, University of Illinois, Urbana, Illinois 61801

(Received 7 October 1968)

Microwave resonant absorption has been observed in OH^--doped KCl and NaCl crystals. Several lines were observed from 8–40 GHz by using relatively standard microwave spectroscopic techniques. The zero-field spectra obtained here indicate that the OH^- ion experiences a strong C_{4v} potential in addition to the expected octahedral crystal field. The C_{4v} potential probably arises from a shift of the OH^- center of mass from the lattice site.

I. INTRODUCTION

ELECTRIC ordering and dielectric relaxation experiments[1,2] have indicated that the OH^- ion is trapped sustitutionally in place of a Cl^- ion in the KCl lattice and that the diatomic ion is aligned along one of the six ⟨100⟩ axes of the crystal. Apparently, the diatomic ion is best characterized as a tunneling librator[3,4] instead of a hindered rotor.[5,6] More recently, paraelectric resonance of the OH^- ion in KCl has been observed at 35,[7] 24,[8] and 9 GHz.[9] The paraelectric resonance technique is a fixed-frequency experiment where a dc electric field is swept until a difference between tunneling states coincides with the fixed microwave frequency. By choosing an appropriate model, one can assign the paraelectric transition and then extrapolate back to the zero external field. Several zero-field models have been proposed[4,10,11] which account for the above paraelectric experiments and also the near- and far-infrared experiments[12–14] and the thermal

† This work was supported by the Advanced Research Projects Agency Grant No. SD-131 to the Materials Research Laboratory at the University of Illinois.

[1] U. Kuhn and F. Luty, Solid State Commun. **2**, 281 (1964); **3**, 31 (1965); **4**, 31 (1956).

[2] I. Shepherd and G. Feher, Phys. Rev. Letters **15**, 149 (1965).

[3] U. Bosshard, R. W. Dreyfus, and W. Känzig, Phys. Kondensierten Materie **4**, 254 (1965).

[4] H. B. Shore, Phys. Rev. **151**, 570 (1966).

[5] A. F. Devonshire, Proc. Roy. Soc. (London) **A153**, 601 (1936).

[6] V. Narayanamurti, Phys. Rev. Letters **13**, 693 (1964). This paper notes that the hindered rotor model is appropriate to the CN^- ion trapped substitutionally in place of the Cl^- ion in KCl.

[7] G. Feher, I. Shepherd, and H. B. Shore, Phys. Rev. Letters **16**, 500 (1966).

[8] L. D. Shearer and T. L. Estle, Compt Rend. **14**, 644 (1966); Solid State Commun. **4**, 639 (1966).

[9] W. E. Bron and R. W. Dreyfus, Phys. Rev. Letters **16**, 165 (1966); Phys. Rev. **163**, 304 (1967).

[10] M. E. Baur and W. R. Salzman, Phys. Rev. **151**, 710 (1966).

[11] W. N. Lawless, Phys. Kondensierten Materie **5**, 100 (1966).

[12] C. K. Chau, M. V. Klein, and B. Wedding, Phys. Rev. Letters **17**, 521 (1966).

[13] B. Wedding, thesis, University of Illinois, 1968, (unpublished); B. Wedding and M. V. Klein, Phys. Rev. **177**, 1274 (1969).

[14] M. V. Klein, B. Wedding, and M. A. Levine, Phys. Rev. **180**, 902 (1969).

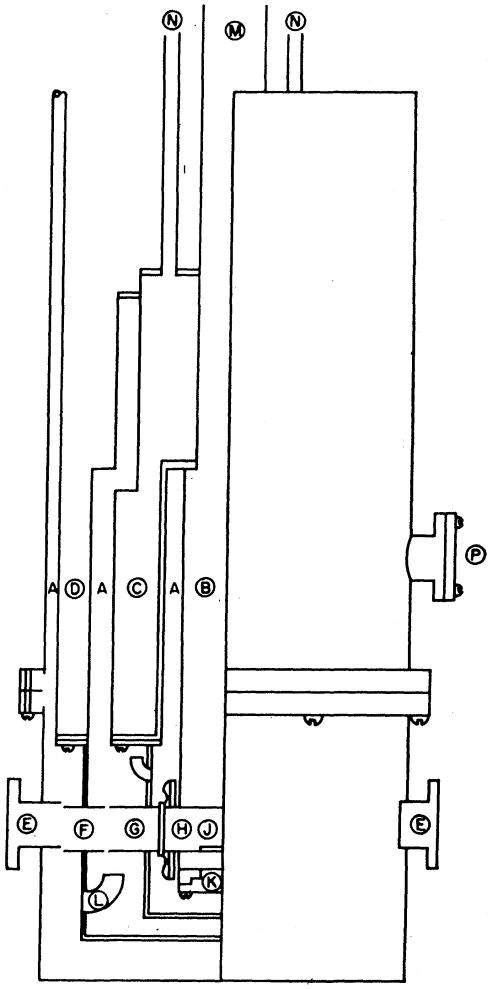

FIG. 1. The cryostat. The letter designations are A, vacuum insulation jacket and spaces; B, pumped liquid-helium container; C, liquid-helium container at 4.2°K; D, liquid-nitrogen container; E, room-temperature microwave flanges; F, liquid-nitrogen radiation shield with waveguide sections; G, liquid-helium radiation shield with waveguide sections; H, Eimac-brazed sapphire windows on annular ring to seal in superfluid helium; J, sample chamber with removable bottom for inserting sample; K, pumped helium chamber port for inserting sample, sealed by crushed indium ring; L, radiation shield interchamber pumping port; M, liquid-helium fill tube for pumped chamber and pumping line; N, fill and vent for liquid-helium shield chamber; and P, vacuum jacket pumping port.

conductivity[15] of the OH^--doped KCl. However, zero-field microwave spectroscopic experiments have not been performed up to this time.

In light of the above background in elucidating the nature of the zero-field interactions of the OH^- ion in KCl, we have investigated the zero-field microwave spectrum of OH^--doped KCl from 8 to 40 GHz. Our results indicate that the zero external field or lattice field experienced by the OH^- ion is not octahedral, as proposed most often by others.

[15] M. V. Klein, Phys. Rev. **141**, 489 (1966).

II. EXPERIMENTAL

Our experiment was modeled after a standard Stark-modulated gas-phase microwave spectrograph. The OH^--doped samples were split along a random axis and a thin conducting film was inserted between the two halves. The conducting film was connected through suitable outlet leads to a zero-based electric field square-wave generator, which serves as a Stark modulator as in gas-phase microwave spectroscopy. This assembly was inserted into a section of x-band waveguide, which was sealed into a cylindrical container with its ends protruding through the wall of the container. During an experimental run, this container was filled with superfluid helium, which also filled the waveguide and cooled the sample. The waveguide ends were sealed by Eimac-brazed sapphire windows, which sealed in the superfluid helium but allowed transmission of microwave energy. This container was the center of a cryostat surrounded by two heat shields, one at 4.2°K and one at 80°K, which made it possible to cool the sample chamber to 1.1°K. The temperature was measured by a Honeywell cryogenic sensor, to an accuracy of 0.05°K, and checked by measuring the vapor pressure of the helium gas in the sample chamber. The waveguide section which contained the sample was modified to allow insertion of the sample through a removable side wall which allowed a high-voltage lead for generating the Stark modulation field. This waveguide section was then coupled through x-band waveguide sections in the heat shields to the outer wall of the cryostat. A schematic of the cryostat is shown in Fig. 1.

The empty but cooled cryostat transmitted microwaves suitably from 8 to 40 GHz. The microwave transmission with the sample immersed in liquid helium was also sufficient to sweep the entire 8–40-GHz region. The microwave signal generator was an Alfred model 650 sweep oscillator and four plug-ins from 8–40 GHz. During an experiment, the sample was maintained at 1.10–1.35°K for a period of about 4 h. This was usually sufficient time to sweep one of the four bands. The microwaves, transmitted through the cell, were detected with standard silicon-crystal detectors and the signal was amplified at the 100-kHz frequency of the high-voltage Stark modulation. The signal was displayed on an oscilloscope or phase-detected and recorded. A block diagram of the Stark spectrometer is shown in Fig. 2. The frequencies were measured with the dial readings on the Alfred sweep oscillator which was calibrated with known gas-phase microwave transitions in a standard microwave spectrograph.[16] The frequencies reported here are accurate to 0.1 GHz. The sweep experiments were tried with an empty cell, with other dielectric materials in place of

[16] The microwave spectrograph which employs this equipment is described in W. H. Flygare, W. Hüttner, R. L. Shoemaker, and P. D. Foster, J. Chem. Phys. **50**, 1714 (1969).

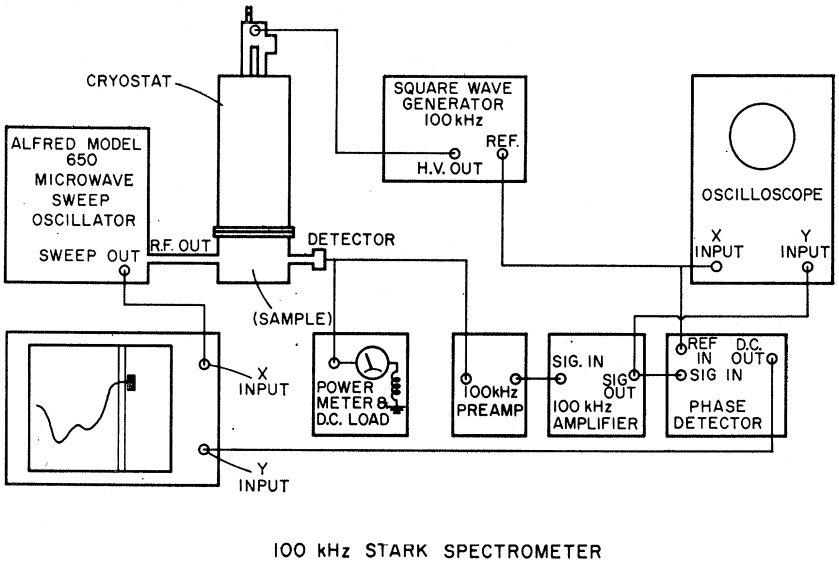

FIG. 2. 100-kHz Stark modulation spectrometer.

the KCl or NaCl crystals and several KCl and NaCl samples with different concentrations of OH^- ions. We observed several microwave absorptions only in OH^--doped KCl and NaCl crystals.

The samples were obtained from Klein.[17] We used samples of Harshaw "pure" KCl, Harshaw "pure" NaCl, chlorine-treated KCl and NaCl, and OD^--doped KCl. The last sample was useful only for the study of concentration dependence. All the samples had a mass of about 20 g and were cleaved to a size that nearly filled the cross section of the waveguide cell. The Stark modulation field was applied parallel to the microwave electric field.

We were not able to transmit a constant power level through the cryostat over a wide range of frequencies due to impedance mismatches in the waveguide system in the cryostat. We were able to use various waveguide tuning techniques to smooth or shift the most severe reflections. The observed resonances characteristically had widths of 50–250 MHz and their response to the narrow power variations made it impossible for us to obtain meaningful Stark spectra. However, we were able to estimate relative intensities to an order of magnitude, and to determine the sign of the Stark effect for all the resonances in spite of the fact that we could not fully modulate them with the Stark fields available.

The spectra observed in KCl:OH and NaCl:OH are recorded in Table I. We saw essentially the same spectra in all samples of each crystal except that in the KCl doped with OH^- and OD^- the resonances were so broad that they formed an absorption continuum. The best sample for the KCl study was the chlorine-treated KCl, which had 0.10 ppm OH^- ion. Line broadening due to OH-OH interaction was at a minimum in this sample, and the sensitivity of the detection system was still adequate for the observation of the OH^- resonance spectra. We were not able to obtain more dilute samples. Since samples sufficiently dilute to exhibit no spectra were not available, we had to base our assignment of the spectra to OH^- ion absorption on the concentration effects shown in Table I. The Harshaw "pure" KCl is known to have an OH^- ion concentration of about 1.5 ppm, and this sample has been the object of other similar studies.[7,8]

TABLE I. Resonances observed in KCl:OH^- and KCl:OD^- and NaCl:OH^-.

Frequency (GHz)	Sample source	Relative intensity	Linewidth (MHz)
	KCl:OH and KCl:OD		
8.35	Harshaw	0.5	150
	chlorine-treated	0.1	50
	KCl:OD^-	1	400
9.5	Harshaw	5	150
	chlorine-treated	0.7	80
	KCl:OD^-	20	800
11.5	Harshaw	10	200
	chlorine-treated	1	100
	KCl:OD^-	50	1000
14.2	Harshaw	1	100
	chlorine-treated	0.2	50
	KCl:OD^-	3	300
20.4	Chlorine-treated	0.01	50
22.3	Harshaw	2	150
	chlorine-treated	0.8	50
	KCl:OD^-	3	400
22.8	Harshaw	0.5	100
	chlorine-treated	0.1	50
33.5	Chlorine-treated	0.02	100
	NaCl:OH^-		
17.7	Harshaw	10	250
	chlorine-treated	0.5	100
26.5	Harshaw	3	300
	chlorine-treated	0.1	100

[17] M. V. Klein, S. O. Kennedy, T. I. Gie, and B. Wedding, Mater. Res. Bull. 3, 677 (1968).

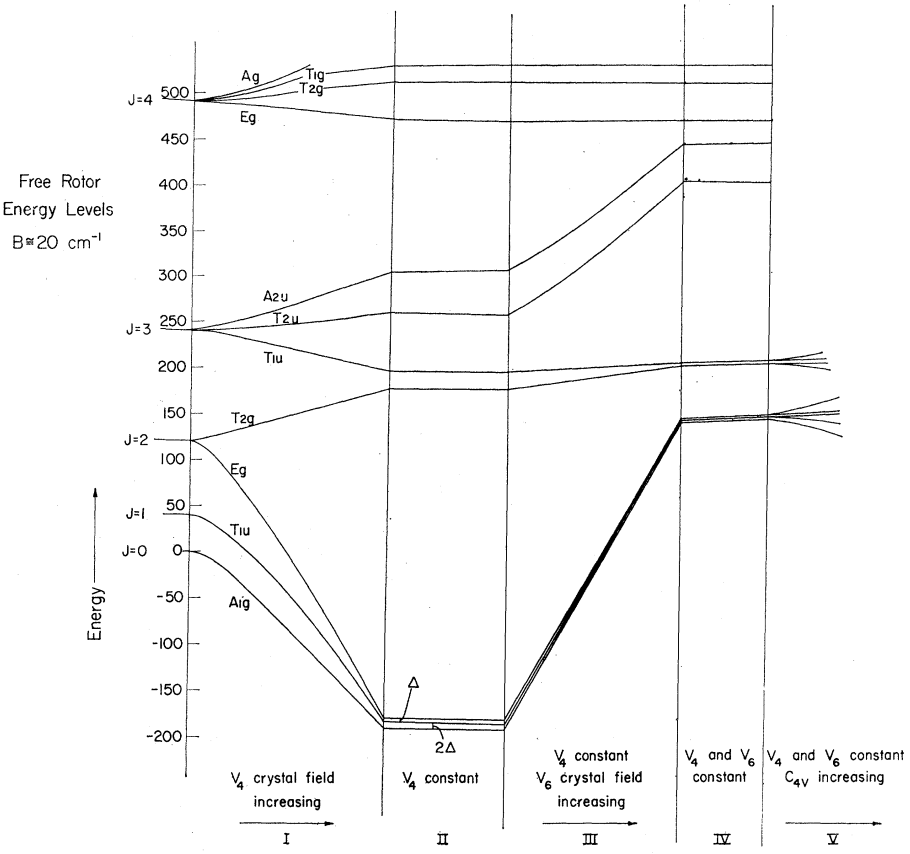

FIG. 3. Correlation diagram between the free rotor and the tunneling vibrator.

The chlorine-treated NaCl has an OH^- ion concentration of about 0.03 ppm. However, we were still able to detect weak absorption in the regions noted in Table I. The Harshaw "pure" NaCl has about 10 ppm OH^- ion making the resonances observed in this sample much stronger and broader. We were unable to obtain samples with OH^- ion concentrations between those of these two samples, and it was obvious from the intensity of the resonances observed in Harshaw "pure" NaCl that more concentrated samples would produce a meaningless continuum of absorption.

The temperature dependence of the resonances produced almost no change in linewidths, but markedly altered their intensities. For KCl:OH, the resonances had essentially disappeared when the temperature reached 4.2°K.

III. THEORY

The tunneling librator as formerly treated assumes that the OH^- ion moves in a potential of octahedral symmetry. As proposed by Shore,[4] the OH^- ion has its center of rotation fixed at the lattice site, is aligned toward one of the positive alkali metal ions, librates or tunnels about this center of rotation, and the energy of the first six states will be arranged in three levels, as previously described.

KCl:OH^- Systems

The spectrum we observed is considerably more complex than the tunneling predicted on the basis of the simple octahedral field with the OH^- ion along one of the six equivalent ⟨100⟩ axes. It is easy to show that Devonshire's[5] hindered rotor model must correlate with the tunneling librator, as shown in Fig. 3. Flygare[18] has discussed the expansion of the potential energy in an octahedral lattice. In general, the potential can be written as[19]

$$V=V_0+V_4+V_6+V_8+\cdots. \quad (1)$$

V_0 is the point charge term and does not effect the rotational or orientational energy of the diatomic ion. V_4 has been discussed in detail by Devonshire.[5] The Devonshire energy levels under the V_4 potential must correlate with Shore's[4] librational model. This correlation is shown in Fig. 3 in region I, where the levels come together in groups of six corresponding to the six $|-x\rangle$, $|+x\rangle$, $|-y\rangle$, $|+y\rangle$, $|-z\rangle$, and $|+z\rangle$ ⟨100⟩ equivalent orientational states in the librational model. Region II shows the librational system, where the splitting between the A_1g and T_1u levels is found to

[18] W. H. Flygare, J. Chem. Phys. 39, 2263 (1963).
[19] See Eqs. (6) and (7) of Ref. 18.

be twice the splitting between the T_1u and Eg levels. Flygare[17] has discussed the V_6 or next nonzero term in Eq. (1) and showed that the V_6 term would not affect appreciably the near-free HCl rotor in the argon lattice. In order to explain the 30-cm^{-1} energy spacing[20] in the KCl:OH$^-$ system, Bauer and Salzman[21] have suggested that the ⟨100⟩ K^+-K^+ axis orientation of OH$^-$ in KCl is not the lowest-energy configuration but instead the H end of the OH$^-$ ion will be at a lower energy point when directed toward the next-nearest-neighbor Cl$^-$ ion. This, in essence, is the influence of the V_6 term in Eq. (1), as discussed by Flygare.[17] If the V_6 term were dominant, there would be 12 equivalent orientations in the lattice and the original rotational states shown in Fig. 1 would begin to group in sets of 12. This is shown schematically in region III of Fig. 3. The V_6 term does not break any of the originally degenerate states under the V_4 term in Eq. (1). Region IV shows the V_4 and V_6 nonzero but constant region.

If the energy levels appropriate to the OH$^-$ ion in KCl were in any of the regions I to IV in Fig. 3 we would only have observed two transitions; $A_1g \rightarrow T_1u$ at approximately 2Δ and $T_1u \rightarrow Eg$ at approximately Δ. The $A_1g \rightarrow Eg$ transition is not allowed under pure octahedral symmetry. However, we observed many more lines, which force us to conclude that the degeneracies of the pure octahedral field have been lifted, as shown in region V of Fig. 3.

If the center of rotation of the OH$^-$ ion (which need not coincide with the center of mass) is not at the lattice site during a rotation or tunneling motion, an apparent C_{4v} perturbation will be present. The V_0 point-charge interaction term in Eq. (1) forces the center of the OH$^-$ ion to the center of the lattice site. However, we are now suggesting that there must be a maximum in energy when the OH$^-$ ion center of rotation is at the lattice site. That is, apparently the OH$^-$ ion is attracted toward the K$^+$ ion due to a charge transfer or some other interaction. As a result of this shift from the lattice site, the octahedral symmetry is broken *as far as the rotational or tunneling motion is concerned.* This apparent C_{4v} perturbation lifts the degeneracies of the original three levels in the over-all octahedral field, as shown schematically in Fig. 3 (region V) and in detail in Fig. 4. The resultant C_{4v} crystal field can be parametrized, as in Shore,[4] to compute the effects on the original octahedral tunneling states.

TABLE II. Assignment of microwave spectra at zero applied field for KCl:OH$^-$. $\Delta = 6.20 \pm 0.10$ GHz. $\gamma_0/\Delta = 1.10$.

Transition	Δ units	Frequency (GHz)	Observed frequency (GHz)
$2A_1$ to $1E$	0.34	2.15	out of range
$1B_1$ to $3A_1$	0.53	3.44	out of range
$1E$ to $1B_1$	1.00	6.20	out of range
$2A_1$ to $1B_1$	1.34	8.34	8.35
$1E$ to $3A_1$	1.53	9.5	9.5
$2A_1$ to $3A_1$	1.87	11.5	11.5
$1A_1$ to $2A_1$	1.85	11.5	11.5
$1A_1$ to $1E$	2.21	13.7	14.2
$1A_1$ to $1B_1$	3.21	20.0	20.4
$1A_1$ to $3A_1$	3.72	22.8	22.8

[20] D. R. Bosomworth, Solid State Commun. **5**, 681 (1967).
[21] M. E. Baur and W. R. Salzman, Phys. Rev. Letters **18**, 590 (1967).

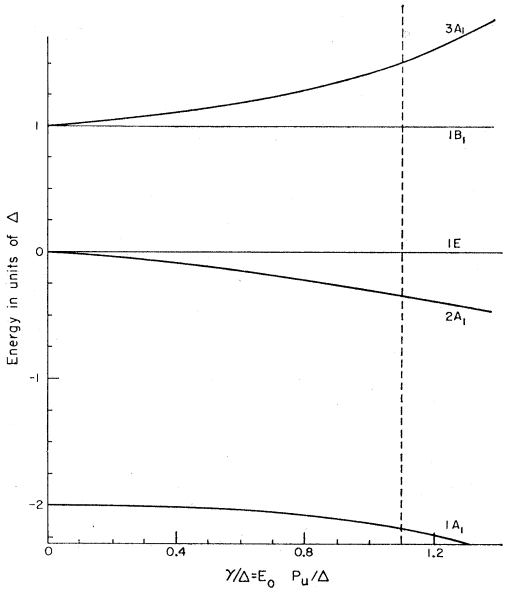

FIG. 4. Energy-level diagram showing the effect of the C_{4v} potential.

Referring to Fig. 4, we can fit our spectra with the two parameters Δ and γ, as shown with the dotted line. The assignments are listed in Table II and the resultant values of Δ and γ are

$$\Delta = (6.20 \pm 0.1)\ \text{GHz}, \quad \gamma/\Delta = 1.10. \qquad (2)$$

The 22.8-GHz resonance is due to a transition shown by Shore[4] to be very weak. The transitions to which the 8.35- and 20.4-GHz resonances are assigned are forbidden by the pure V_4 model. However, simultaneous presence of V_6, C_{4v}, potentials, and the Stark field will cause $A_1 \rightarrow B$ transitions to be allowed.

It has been shown that other dipole sites such as Li$^+$ and HCl can interact with an external electric field[22,23] and can produce paraelectric resonance[24,25] in the KCl crystal. The same site could then absorb in the microwave region and could be the cause of our unassigned resonances.

In the above approach and analysis we have assumed that the translational motion leading to tunneling of the OH$^-$ center of mass from one energy minimum to

[22] H. S. Sack and M. C. Moriarity, Solid State Commun. **3**, 93 (1965).
[23] G. Lombardo and R. O. Pohl, Phys. Rev. Letters **15**, 291 (1965).
[24] D. Hocherl, D. Blumenstock, and H. C. Wolf, Phys. Letters **24A**, 511 (1967).
[25] G. Hocherl and H. C. Wolf, Phys. Letters **27A**, 133 (1968).

another is slow relative to the rotational motion at a fixed point in the lattice. We attribute the existence of the several energy levels to an effective break with O_h symmetry due to the off-center rotation of the OH^- ion. Another approach would be to assume that the rotational motion is slow relative to the translational motion from one minimum to another. This model of strong translational-rotational interaction[26] was necessary to explain the complex motion in the Ar:HF system[26] which is isoelectronic to the KCl:OH^- system studied here. We have attempted unsuccessfully to explain our KCl:OH^- data on the basis of the translational model.[26] Furthermore, the off-center rotor seems more reasonable for the KCl:OH^- system on the basis of relaxation experiments[27] and the mass dependence of the infrared vibration.[14]

Our zero-field value of γ is equivalent to an application of an [100] external electric field E on an electric dipole p_u to give $Ep_u/\Delta=1.10$, as shown by Shore.[4] Thus, we find an octahedral tunneling frequency parameter Δ which is in remarkable agreement with the value obtained by extrapolation by Feher, Shepard, and Shore[7] by paraelectric resonance with the external electric field along the [100] axis. However, Feher, Shepard, and Shore have obtained the OH^- dipole moment by extrapolating their high-field 35.2-GHz transition from Fig. 4 back to $\gamma/\Delta=0$. If their result is extrapolated back to the internal field of $\gamma/\Delta=1.10$, a dipole moment of 2.2 Debye units is found. This analysis is consistent with the other paraelectric resonance work. The 24.5-GHz work of Shearer and Estle,[8] with the applied electric field in the [100] direction, done at 24.5 GHz, is also consistent with our assumption if a dipole moment of 1.9 Debye units is assumed. The same consistency is found for the [100] orientation work by Bron and Dreyfus[9] at a frequency of 9.1 GHz, with a somewhat lower dipole moment. Similar results are obtained by comparing our model with the [111] and [110] paraelectric resonance work.[28] That is, for an applied electric field in the [111] direction, this perturbation was added to a fixed perturbation $\gamma=E_0p_u=1.10\Delta$, aligned along the [100] direction; and this total perturbation was added to the octahedral potential energy-level diagram.[28] The energy levels obtained were quite consistent with the published work of the three groups previously discussed when a dipole moment of about 2.2 Debye units is assumed for the OH^- site. Olny Shearer and Estle[8] report transitions with an electric field applied along the [110] direction. These transitions can be fit to a composite energy-level diagram for this orientation when a dipole moment of 2.1 Debye units is assumed.[28]

The over-all result of our interpretation of the reported paraelectric resonance spectra is that there is more consistency in the calculation of the dipole moment when these spectra are referred to energy-level diagrams resulting from our model than when they are referred to energy-level diagrams assuming a zero-field octahedral potential.

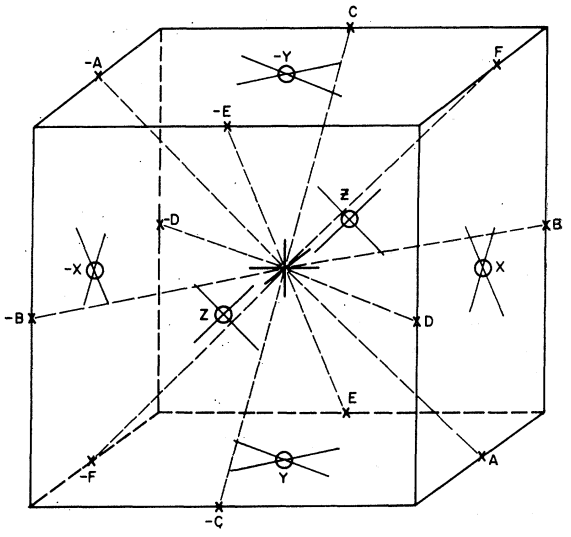

FIG. 5. NaCl lattice showing the tunneling states corresponding to the different next-nearest-neighbor orientations.

NaCl:OH^- System

We will attempt to show here that the NaCl:OH^- system falls under the same $V_4+V_6+C_{4v}$ model as discussed above for KCl:OH^-. As we only observed two transitions in the NaCl:OH^- system we cannot obtain a unique fit of the data to the energy-level diagram in Fig. 4. However, $\gamma/\Delta=1.1$ and $\Delta=49$ GHz will fit our observed data by analogy to the KCl:OH^- system. At this point in our work, the experimental results of the far-infrared investigation performed by Kirby, Hughes, and Sievers[29] were made available to us. We were able to combine these spectra with the microwave spectra to make a complete assignment to the energy-level diagram predicted by our C_{4v} model, and we were able to extend this model to the first set of excited librational levels.

A sideband on the near-infrared spectra of OH^- ion in alkali halide crystals assigned to the OH^- librator has been regarded as an anomaly.[12] These sidebands, which in KCl:OH^- is displaced by 30 cm^{-1} and in NaCl:OH^- is a structured band centered at 14 cm^{-1}, have been observed directly in the far infrared by Bosomworth[20] and Kirby *et al.*,[29] respectively.

We will now attempt to show that the features of both KCl:OH^- and NaCl:OH^- will fit into the general energy-level diagram shown in Fig. 3. The general idea

[26] M. T. Bowers, G. I. Kerley, and W. H. Flygare, J. Chem. Phys. **45**, 3399 (1966).
[27] F. Luty, J. Phys. (Paris) **28**, Suppl. C-4, 120 (1967).
[28] The details of these calculations are given in R. S. Scott, thesis, University of Illinois, 1968 (unpublished).
[29] R. D. Kirby, A. E. Hughes, and A. J. Seivers, Phys. Letters **28A**, 170 (1968).

is that the energy levels are described by region V in Fig. 3, where the approximate spacing between the lower six and the next highest six levels is about 30 cm^{-1} in KCl:OH^- and 15 cm^{-1} in NaCl:OH^-. In the previously discussed KCl:OH^- system, we localized our discussion to a dominant V_4 term and smaller V_6 and C_{4v} effects. We will attempt to show in NaCl:OH^- that the V_6 term enjoys a larger relative importance than in KCl:OH^-.

Shore[4] has considered the dominant V_4 term, which is caused primarily by the six nearest neighbors. We will now consider a dominant V_6 term caused primarily by the 12 nearest neighbors. Following Shore[4] we label the 12 orientations for the hetronuclear diatomic OH^- ion as indicated in Fig. 5. It is clear from Fig. 5 that there are four possible types of tunneling motion. Choosing the state $|A\rangle$ as a starting place, there is the motion to state $|B\rangle$ through an angle of 60°, the motion to state $|F\rangle$ through an angle of 90°, the motion to state $|C\rangle$ through an angle of 120°, and the motion to state $|-A\rangle$ through an angle of 180°. These state functions have the same properties discussed earlier[4] for the functions used as the basis set for the V_4 model Hamiltonian. The potential-allowing tunneling is referred to as V_{16} and its matrix elements are defined as $\langle A|V_{16}|F\rangle=\langle A|V_{16}|F\rangle=-\frac{1}{2}\alpha$ and $\langle A|V_{16}|C\rangle=\langle A|V_{16}|-A\rangle=0$, which means that tunneling through 60° or 90° is allowed with equal probability, but that tunneling through 120° or 180° is not allowed. These assumptions are compatible with those used by Shore[4] in his work with six nearest neighbors. Using the 12 basic functions for the next-nearest neighbors and the potential matrix elements defined for V_{16}, we generated the model Hamiltonian matrix:

	A	B	C	D	E	F	$-A$	$-B$	$-C$	$-D$	$-E$	$-F$
A	0	1	0	1	1	1	0	0	1	0	0	1
B	1	0	1	1	1	1	0	0	0	1	0	0
C	0	1	0	0	1	1	1	0	0	1	1	0
D	1	1	0	0	0	1	0	1	1	0	1	0
E	1	1	1	0	0	0	0	0	1	1	0	1
F	1	1	1	1	0	0	1	0	0	0	1	0
$-A$	0	0	1	0	0	1	0	1	0	1	1	1
$-B$	0	0	0	1	0	0	1	0	1	1	1	1
$-C$	1	0	0	1	1	0	0	1	0	0	1	1
$-D$	0	1	1	0	1	0	1	1	0	0	0	1
$-E$	0	0	1	1	0	1	1	1	1	0	0	0
$-F$	1	0	0	0	1	0	1	1	1	1	0	0

$\times\frac{1}{2}\alpha J$ (3)

Diagonalizing this matrix gives the 12 energy levels:

energy	state	degeneracy
2α	T_1u, T_2g	6
α	Eg	2
0	T_1u	3
-2α	A_1g	1

The T_1u and T_2g degeneracy is broken under the influence of V_4 in considering the nearest neighbors. This degeneracy is also broken by allowing 120° or 180° tunneling. Adding the C_{4v} perturbation to the above model given the same states as discussed with V_4 previously.

Figure 6 shows an enlarged view of region V in Fig. 3, which is a composite of the $V_4+V_6+C_{4v}$ potentials. We assign the far-infrared spectra observed at 30 cm^{-1} in KCl:OH^- and the structured bond around 14 cm^{-1} for NaCl:OH^- as transitions between the lowest six and next-highest six energy levels, as shown in Figs. 3 and 6. The relative importance of the next-nearest neighbors is higher in the NaCl:OH^- system, leading to a closer relative grouping of the two sets of six levels. The 30-cm^{-1} spectra for KCl:OH^- showed no resolvable structure, as would be expected considering the small value of Δ for the tunneling levels of that system and the limitations on the resolving power of a far-infrared spectrometer. However, our assignment of the microwave spectra from NaCl:OH^- led to a much larger value for Δ placing the energy between transitions within the resolving ability in the far infrared. Therefore, we expected that the structure of the far infrared spectra due to the NaCl:OH^- would be resolvable and assignable to our model. This assumption is confirmed by the experimental data reported by Kirby, Hughes, and Sievers,[29] and our assignment of their data along with our microwave data is shown in Fig. 6 and in Tables III and IV. While the temperature dependence of the microwave spectra showed both lines

TABLE III. Assignment of the far-infrared spectra to the model shown in Fig. 6.

Far-infrared absorbtion (cm^{-1})	Assignment
2	$2A_1$ to $1B_1$ or 1E to $3A_1$
9.3	$3A_1$ to $2T_1$
10.2	$1B_1$ to $2T_1$
12.2	$2A_1$, 1E to $2T_1$
15.7	$1A_1$ to $2T_1$
22	$3A_1$ (others) to $2T_2$

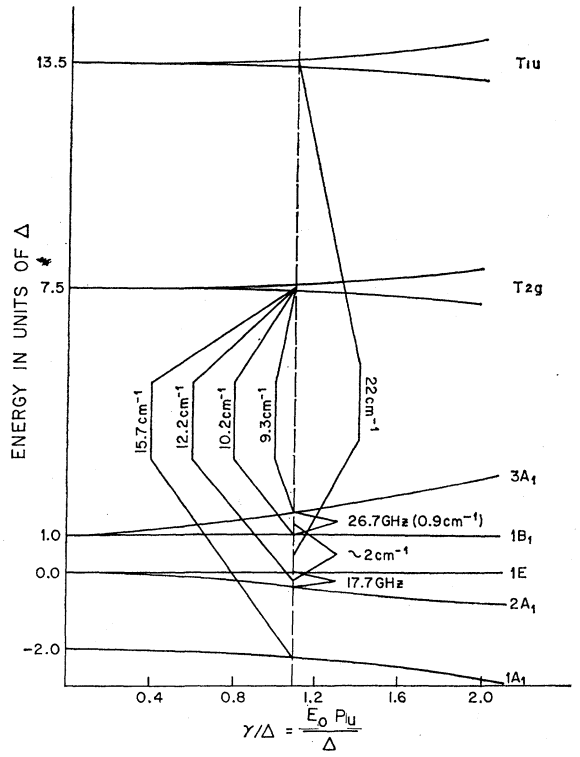

FIG. 6. Energy-level diagram showing the lowest 12 levels and the assignments to the microwave and far-infrared data.

decreasing in intensity with an increase in temperature as expected, the temperature dependence of the far infrared shows trends which are predictable from the assignment. At 4.2°K, the 9.3-cm^{-1} line is most intense while the 15.7-cm^{-1} line is least intense and all lines in between decrease in intensity with increasing frequency. At 1.4°K, the intensity of the 9.3-cm^{-1} line has decreased while that of the 15.7-cm^{-1} line has increased and the intermediate lines have intensities more nearly equal. At 0.6°K, the 9.3-cm^{-1} line is very weak while the 15.7-cm^{-1} lines is very strong and the lines in between have increasing intensity with increasing frequency. The line at 22 cm^{-1} is not observed at the lowest temperature and is most intense at the highest temperature. The 2-cm^{-1} band is only observed at 1.4°K, where there is sufficient population of the upper tunneling levels to absorb radiation, and sufficient population difference between these levels to produce strong absorption. While it should have been possible for these investigators to resolve a line due to the predicted 6.5-cm^{-1} transition from $1A_1$ to $3A_1$, Shore[4] has shown that this transition is very weak.

TABLE IV. Assigned energy transitions between the lower six levels shown in Fig. 6.

Transition	Frequency (GHz)	Frequency (cm^{-1})	Observation: Microwave (GHz)	Observation: Far-infrared (cm^{-1})
$1B_1$ to $3A_1$	27	0.9	26.5	10.2– 9.3
1E to $3A_1$	76	2.5	out of range	12.2–10.2 2
$2A_1$ to $1B_1$	66	2.2	out of range	12.2–10.2
$2A_1$ to $3A_1$	93	3.1	out of range	12.3– 9.3
$2A_1$ to 1E	17.5	0.6	17.7	out of range
$1A_1$ to $3A_1$	195	6.5	out of range	15.7– 9.3

IV. CONCLUSION

The main conclusion of this work is that the electrostatic potential energy of interaction between the OH^- ion and the lattice in both the NaCl:OH^- and KCl:OH^- systems is less than octahedral in symmetry. We propose here a model which involves the interaction between the OH^- ion and the six nearest-neighbor positive ions and the 12 next-nearest-neighbor negative ions. In addition, we assume that the center of rotation is off the lattice site and that the rotational or tunneling motion takes place off the lattice site and without the corresponding translational motion. This model apparently is capable of explaining our observed zero-field data, the paraelectric resonance work, and the near- and far-infrared spectra of the KCl:OH^- and NaCl:OH^- systems.

The OH^- ion in NaCl experiences stronger OH^--Cl^- next-nearest-neighbor interactions than the OH^- ion in KCl. Thus, even though the nearest-neighbor interactions in NaCl are larger than in KCl, the effective potential in NaCl is more nearly spherical due to strong next-nearest-neighbor interaction. Thus, the tunneling frequencies in the NaCl:OH^- system are larger because of the lower relative barriers between the potential minima. The stronger relative next-nearest-neighbor interactions in NaCl also force the lower six tunneling states closer to the next-highest six tunneling states leading to a lower-frequency far-infrared spectrum than in the corresponding KCl:OH^- system.

ACKNOWLEDGMENTS

We are indebted to Professor M. V. Klein for the use of his samples and for many helpful discussions. Dr. John Zahrt provided helpful suggestions.